

HIGH-POWER TESTS OF A REMOTE STEERING LAUNCHER MOCK-UP AT 140 GHZ

G. Gantenbein¹, W. Kasperek¹, B. Plaum¹, K. Schwörer¹, M Grünert¹, V. Erckmann², F. Hollmann², L. Jonitz², H. Laqua², G. Michel², F. Noke², F. Purps², A. Bruschi³, S. Cirant³, F. Gandini³, A.G.A. Verhoeven⁴, ECRH groups at IPP Greifswald², FZK Karlsruhe⁵ and IPF Stuttgart¹,

¹Institut für Plasmaforschung, Universität Stuttgart, Pfaffenwaldring 31, D-70569 Stuttgart, Germany

²Max-Planck-Institut für Plasmaphysik (IPP), EURATOM-Association, D-17491 Greifswald, Germany

³Instituto di Fisica del Plasma, EURATOM-ENEA-CNR Association, via R Cozzi 53, 20125 Milano, Italy

⁴FOM Institute for Plasma Physics Rijnhuizen, Association EURATOM-FOM, Nieuwegein, The Netherlands

⁵Forschungszentrum Karlsruhe, Association EURATOM-FZK, IHM, D-76021 Karlsruhe, Germany

e-mail: gantenbein@ipf.uni-stuttgart.de

Introduction

The next major step in the development of tokamaks towards fusion power plants will be the International Thermonuclear Experimental Reactor (ITER). This machine will be equipped with an electron cyclotron resonance heating (ECRH) system which can be applied for very localised heating of the plasma or for current drive (ECCD) in the plasma [1]. One major objective of this system is the suppression of plasma instabilities, particularly the so-called neoclassical tearing modes (NTMs) which are very likely to appear in current operating scenarii of ITER. These modes are excited on different rational surfaces, but the modes $(m/n) = (3/2)$ and $(2/1)$, where m is the poloidal and n the toroidal mode number, respectively, are considered to be the most dangerous ones. The occurrence of the modes at different locations requires a flexible tool in order to react on the specific mode during the discharge. To deposit the ECRH power at different rational surfaces it is necessary to sweep the beam in the poloidal direction. The present launcher concept which is foreseen to fulfill this task is the so-called remote steering launcher. Its main technical advantage is that moveable parts close to the plasma are completely avoided while the injection angle of the beam into the plasma is adjusted several meters away from the plasma [2].

The launcher concept is based on the imaging properties of square waveguides of a certain length $L_B = 4a^2/\lambda$ where a is the waveguide inner width and λ the vacuum wavelength. The propagation constant for $TE_{m,n}$ modes in a waveguide

with square cross section is given by $k_{m,n} = k_0(1 - (m^2 + n^2)\lambda^2/4a^2)^{1/2}$, where k_0 is the propagation constant in vacuum. For low order modes ($m\lambda/2a$ and $n\lambda/2a \ll 1$) $k_{m,n}$ can be approximated by $k_{m,n} \approx k_0(1 - (m^2 + n^2)\lambda^2/8a^2)$. This shows that the propagation constants of the modes differ by a multiple of $\Delta k = \pi\lambda/(4a^2)$ and hence the phase difference δ of adjacent modes is an odd multiple of π for a waveguide length of $L = L_B$. Thus, an antisymmetric image of the field distribution at the waveguide entrance is reproduced at the end of the waveguide. However, for large scanning angles higher order terms contributing to δ become important. They result in a phase slippage of the waveguide modes in the form $\Delta\delta \approx k a \phi^3 (n_1 - n_2)$ which limits the useful scanning angle range [3].

Figure 1 shows the calculated TEM_{00} power in the wanted direction (Note: the power losses due to Ohmic heating are much lower). This example shows that the mode purity is high ($> 90\%$) for scanning angles up to 10° . For higher angles the power in the main beam is strongly decreasing and a beam in the opposite direction develops.

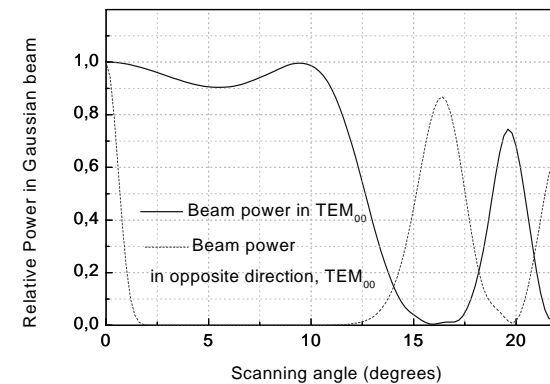


Figure 1: Efficiency of the TEM_{00} beam in nominal and opposite direction vs scanning angle. Note that power in higher-order modes in this calculation is considered as loss (from [4]).

In an earlier work results of low-power measurements on a square waveguide in the frequency range 140 – 160 GHz were presented [3]. This contribution reports on first high power experiments with a straight square waveguide at 140 GHz (high-power tests at 170 GHz are given in [5]). In the following we will describe the experimental set-up and present some results.

Experimental set-up

The experiments have been carried out using the installations foreseen for the stellarator W7-X which is currently under construction in Greifswald, Germany [6]. A Gaussian beam is produced by a gyrotron at 140 GHz. This gyrotron is capable of delivering a power of up to 1 MW at a pulse length of up to 5 s and 470 kW at a pulse length of up to 180 s [7].

The transmission path from the gyrotron to the waveguide is given in Fig. 2. The complete transmission line of the ECRH system of W7-X is made of reflecting mirrors and is operated under atmospheric pressure, all standard components are designed for cw operation and are watercooled. In front of the square waveguide we have introduced two (uncooled) mirrors which adapt the beam parameters and allow steering of the input beam in the horizontal direction while guiding the beam to the center of the waveguide entrance. One segment of the square waveguide consists of four corrugated walls, each 0.5 m long, screwed and fixed together. The total length of the waveguide is $L_B = 6.62$ m, the inner width is $a = 60.08$ mm, the inner walls have a corrugation with periodicity $p = 0.7$ mm,

depth $d = 0.45$ mm and groove width $w = 0.4$ mm. The RF power is measured with a load which is placed at the end of the waveguide [8], alternatively short pulses are fired on an absorbing screen placed at a distance of about 2 m from the waveguide end.

The thermographic image of the beam on the absorbing screen and the heating of the waveguide wall during a long pulse shot has been recorded with an IR camera. Thermal sensors (PT100) are mounted in the side wall of the first section of the waveguide, close to the inner wall to monitor the temperature increase in the region of the highest heat load (see Fig. 3). Fast optical detectors are used at the entrance and output of the waveguide to provide a shut down signal for the gyrotron in case of arcing.

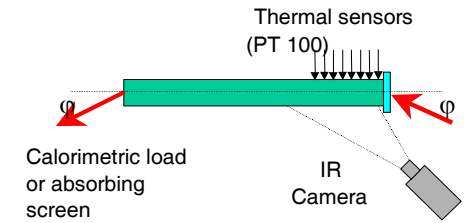


Figure 3: Experimental set-up to observe the heating of the side wall of the waveguide with an IR camera.

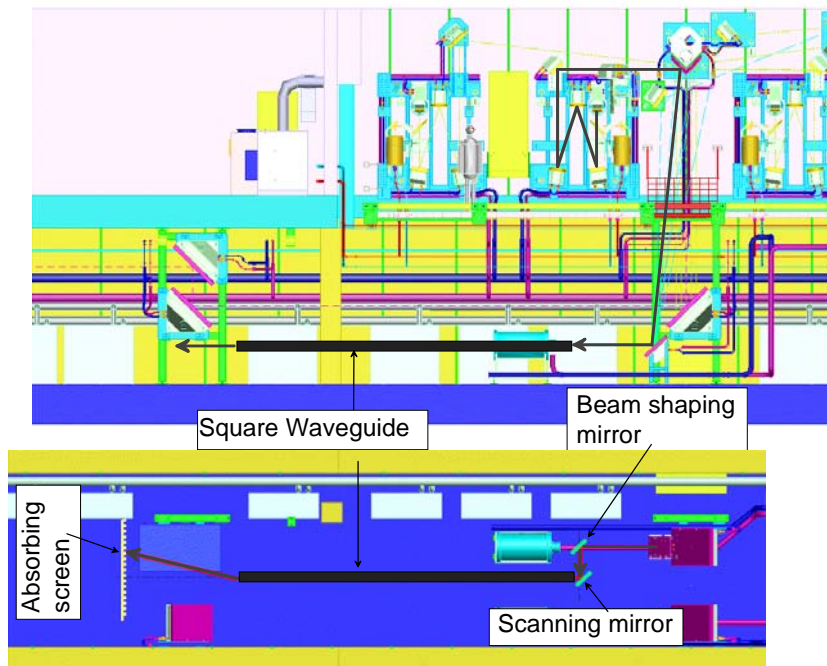


Figure 2: Installations and beam path from gyrotron to square waveguide. The power is transmitted in a quasi-optical line, including polarisers which allow any linear and circular polarisation. The beam power is absorbed in a calorimetric load at the end of the waveguide (not shown here) or on an absorbing screen.

Experimental Results

Several pulses have been performed with a pulse length of up to 10 s and a typical power of ≈ 500 kW. The scanning angle has been varied from $\varphi = 0^\circ$ to 12° , the polarisation was linear, either parallel or perpendicular to the scanning plane. In spite of the fact that the waveguide was operated at normal atmospheric pressure no limitation due to arcing in the waveguide was found.

An example of a measurement with an IR camera is given in Fig. 4. It shows the rectified image of the temperature distribution on the outer surface of the waveguide and a calculation of the power distribution on the inner waveguide wall. Both are in good agreement.

Figure 5 shows the temperature increase at the first reflection of the beam measured with the thermal sensors in a 5 s shot at a scanning angle of 11.6° and perpendicular polarisation. Four elements of each row (central, top and bottom) are given. These data can be used to obtain a rough estimation of the Ohmic losses. Simple integration of this temperature distribution gives the following values for the losses at the first reflection in parallel ($P_{\text{Loss,II}}$) and perpendicular ($P_{\text{Loss,I}}$) polarisation: $P_{\text{Loss,II}} = 0.9$ kW, $P_{\text{Loss,I}} = 0.3$ kW. This has to be compared with laboratory measurements in a precise 3-mirror set-up [9]. For the corrugated wall the ratio of the absorption coefficient of parallel and perpendicular polarisation was measured to be around 3.5 at the respective angle of incidence. The absorption in the waveguide wall can be used to calibrate the calculated angular dependance of the total Ohmic losses of the waveguide. This results in the following approximate formulae: $P_{\Omega,II} \approx 0.033 \varphi^2$ [$^\circ$, %], $P_{\Omega,I} \approx 0.01 \varphi^2$ [$^\circ$, %]. Far-field pattern of the radiated beam on a absorbing screen have been monitored with the IR camera at a distance of 2.175 m from the end of the waveguide. The

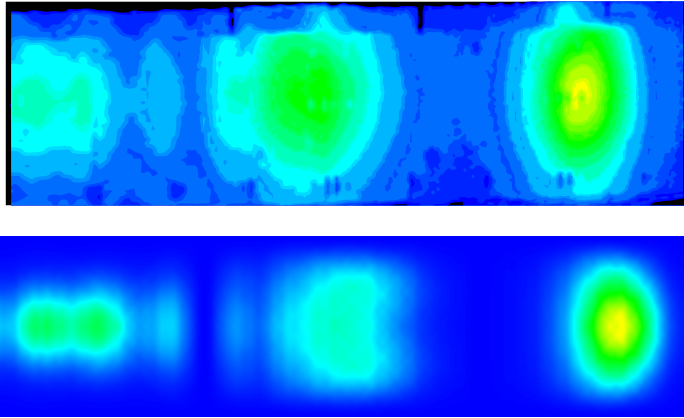


Figure 4: Measured temperature distribution at the outer surface of the waveguide (top) and calculated power distribution at the inner surface (bottom).

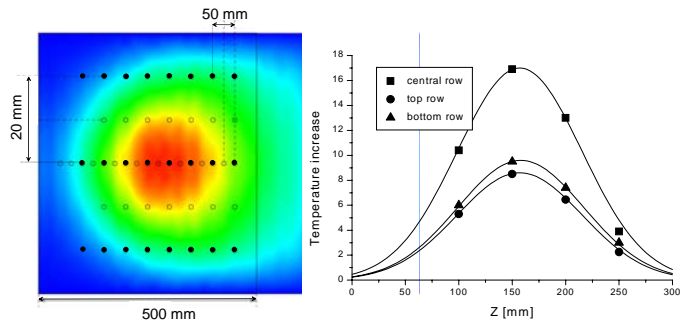


Figure 5: Position of thermal sensors (left) and measured temperature distribution at the end of a 5 s shot.

scanning angle has been varied from 0° to 20° . To avoid the damage of the target the power and pulse length had been reduced to 250 kW and 0.3 ms, respectively. Three shots with 0° , 10° and 12° are given in Figure 6. They show a good qualitative agreement with the low power measurements (see Figure 6). A single beam is observed up to 12° with a low side lobe level, for higher angles (e.g. 15°) the output beam is splitted in two beams with a power ratio which is close to the low power result.

Summary

High-power tests of a remote steering launcher system have been performed successfully with a four-side corrugated square waveguide operated under atmospheric pressure. The maximum values with respect to pulse length, mm-

wave power and injection angle were: $t = 10$ s, $P = 660$ kW and $\varphi = 20^\circ$. In all described operating regimes, no arcing was observed. The results are in good qualitative and quantitative agreement with low power measurements and results at 170 GHz in an evacuated waveguide [5].

This work was carried out under the EFDA technology research programme activities, EFDA technology task TW3-TPHE-ECHULB6. The ECRH for W7-X is built up in the frame of the project PMW hosted at FZK Karlsruhe (collaboration between FZK Karlsruhe, IPP Garching and Greifswald, and IPF Stuttgart).

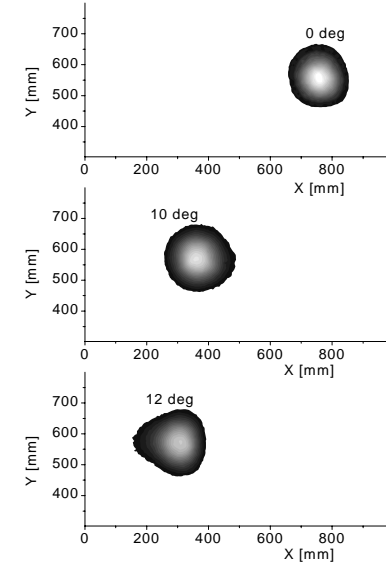


Figure 6: Far field pattern at a scanning angle of 0° , 10° and 12° . Shown is the temperature increase at the target in a linear scale ($\Delta T_{\text{Max}} \approx 11$ °C).

References

- [1] H. Zohm, Proc. of the 13th Joint Workshop on ECE and ECRH, May 2004, Nizhny Novgorod, Russia, <http://www.ec13.iapras.ru/>
- [2] A.G.A. Verhoeven et.al., Proc. of the 13th Joint Workshop on ECE and ECRH, May 2004, Nizhny Novgorod, Russia, <http://www.ec13.iapras.ru/>
- [3] W. Kasperek et al., Nucl. Fusion **43** (2003), 1505 - 1512.
- [4] K. Ohkubo et al., Fusion Engineering and Design, **65** (2003), 657-672.
- [5] K. Takahashi et al., Fusion Eng. and Design, **65** (2003), 589-598.
- [6] Kasperek, W. et al., in "Strong Microwaves in Plasmas 1999", ed. A.G. Litvak, Inst. of Applied Physics, Nizhny Novgorod (1999), 185 - 204.
- [7] G. Dammert et al., IEEE Trans. Plasma Science., **30** (2003), 808-818.
- [8] A. Bruschi et.al., Nucl. Fusion **43** (2003) 1513-1519.
- [9] R. Wacker, private communications.